Membrane Bound Hydraphiles Facilitate Cation Translocation

Goundla Srinivas,* Carlos F. Lopez, and Michael L. Klein

Center for Molecular Modeling, Department of Chemistry, University of Pennsylvania, Philadelphia, Pennsylvania 19104-6323

Received: October 2, 2003; In Final Form: February 2, 2004

The mechanism of hydraphile assisted cation translocation across a lipid bilayer is investigated by means of coarse-grain molecular dynamics simulations. We find that hydraphiles with appropriate length adopt a channel-like conformation in agreement with recent experimental studies. In trans membrane conformation, hydraphiles assist ion-passage across the bilayer via a mechanism that is found to be rare but effective. The observed time for ion translocation is approximately 0.3 ns. Trajectory studies reveal that the translocating ion shows relatively less mobility in the vicinity of the hydraphile ring when compared to that in bulk water. The present coarse grain simulations confirmed that hydraphile molecules with a chain length matching the bilayer thickness can assist ion transport, whereas hydraphiles having a shorter or longer chain length fail to do so. In addition, the present simulation study underscores the necessity of a polar central relay for a molecule to act as a translocation facilitator.

Ion channels play a crucial role in cell functioning by maintaining salt concentration in appropriate proportions in intra- and extracellular domains.[1,2] Certain naturally occurring proteins spontaneously self-assemble in biological membranes to form ion channels with important physiological functions.[1,2] Others serve as powerful naturally occurring antibacterial agents.[3−7] For example, a large number of naturally occurring peptides such as gramicidin, alamethicin, and magainin are reported to show channel forming antibiotic activity.[8,9] Attempts to mimic this functionality have resulted in entirely new classes of synthetic materials.[8−14] Recently, Gokel et al.[15,16] reported that so-called "hydraphiles" also exhibit antibacterial activity. Hydraphiles are based on a three-macrocycle concept; three connected 18-crown-6 cyclic ether rings exhibit channel activity when inserted in a phospholipid bilayer. Experiments[16] suggest a membrane-spanning channel-like role for the hydraphile in ion transport rather than a carrier mechanism. However, the detailed mechanism of action is not well understood.[15,16]

In this study we aim to better understand the hydraphile ion transport mechanism by carrying out a computer simulation study. The time scale for ion translocation across a biological membrane is typically too long to be conveniently studied via computer simulations based on fully atomistic models.[17−21] On the other hand, implicit models can only capture semiquantitative aspects. Hence, an intermediate methodology that is simple enough to cover the desired long time and length scales, yet reliable enough to obtain quantitative information is an ideal choice for this kind of problem. Recently, Klein and co-workers have developed a coarse-grain (CG) model for phospholipid membranes. They have shown that the CG method is efficient enough to study various structural and dynamical aspects of lipid membranes.[22−24] Marrink and Mark also demonstrated the efficiency of the CG method by studying a variety of membrane phenomena.[25−28] These studies were based on pioneering works of Smit et al.[29,30] Encouraged by such studies, in this work we extend the CG model to allow us to probe the ion translocation mechanism across a lipid bilayer. Accordingly, in this study we model both the lipid bilayer−hydraphile system using the CG approach.

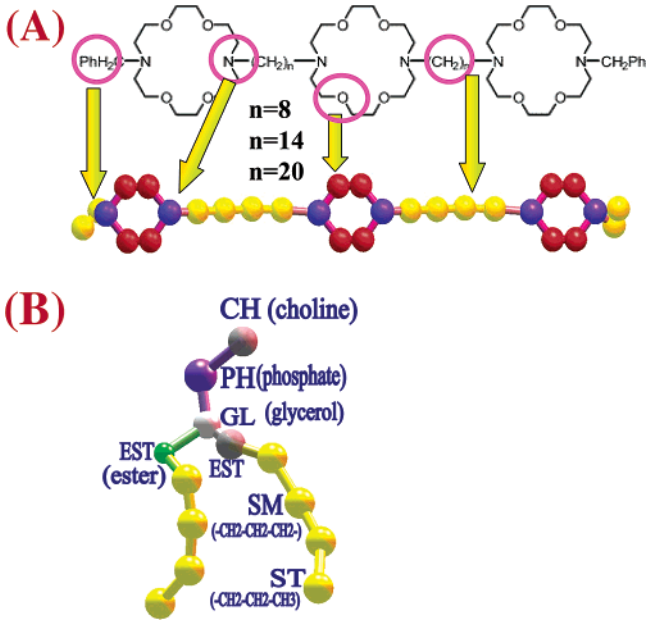

Figure 1. (A) Shown is the mapping of a hydraphile molecule onto a coarse grain model. Hydrophilic 18-crown-6 rings are represented by 6 sites: red spheres are $-CH_2-O-CH_2-$ (symbol-HEST), and blue, $-N-(CH_2)_3$ (symbol-HTMA). Yellow spheres (HSM sites) represent hydrophobic moieties. For the hydrocarbon chain linkers they are $-CH_2-CH_2-CH_2-$. Thus linkers with 8, 14, and 20 carbon atoms, contain two, four, and six SM sites, respectively. We denote these three CG hydraphiles by HY2, HY4, and HY6, respectively. Terminal hydraphile phenyl rings are each represented by two SM sites. (B) CG representation of a DMPC lipid. Representation of the CG units is shown in figure and the corresponding interaction potential parameters are listed in Table 1.

The hydraphile molecule in question has three 18-crown-6 rings, one at each end and one in the middle, which are linked by linear hydrocarbon chains (shown in Figure 1). The length of the linking chains has been shown to affect activity.[15] It has

* Corresponding author. E-mail: srini@cmm.upenn.edu.

10.1021/jp036953b CCC: $27.50
Published on Web 03/16/2004

TABLE 1: Mutual Interaction Parameters among the Various Coarse-Grain Sites Used in This Study[a]

	CH		PH		GL		EST		SM		ST	
sites	σ (Å)	ϵ (K)	σ (Å)	ϵ (K)	σ (Å)	ϵ (K)	σ (Å)	ϵ (K)	σ (Å)	ϵ (K)	σ (Å)	ϵ (K)
HTMA	Tab	Tab	Tab	Tab	Tab	Tab	Tab	Tab	5.5	50	5.50	50
HSM	5.50	50	5.20	40	4.30	70	4.30	70	4.80	178	4.85	218
HEST	Tab	Tab	Tab	Tab	Tab	Tab	Tab	Tab	4.30	70	4.30	70

[a] "Tab" indicates that the tabulated potentials are used for interaction between corresponding species and are plotted in Figure 2. Interaction parameters for the DMPC lipid are obtained from our earlier study.[24]

been postulated that the hydraphiles insert into a lipid membrane with terminal rings at the inner and outer lipid−water interfaces to act as entry and exit portals for cations, with the middle ring necessarily in the hydrophobic region of the bilayer, serving as a "polar central relay".[15,16]

All molecular dynamics (MD) simulations in this work employ the CG model for a fully hydrated bilayer of dimyristoylphosphatidylcholine (DMPC), in which the lipid is represented by the 13 CG sites shown in Figure 1(B). The CG model for water (W) involves groups of three molecules. The effective time scales accessible in this study are estimated to be typically 2 orders of magnitude larger than those in all-atom simulations.[24,25]

In our previous studies, we have developed a coarse-grain model for DMPC lipids.[24] Hence, we skip the parametrization details in this paper and present only the important aspects of the coarse grain methodology and the final parameters. Briefly, the coarse-grain (CG) parameters have been developed by obtaining selected target observables either from experiments or by carrying out all atom simulations of corresponding species. The present CG DMPC model has been used earlier to study variety of membrane phenomena, including structural and dynamical aspects,[24,25] and membrane fusion.[26]

In Figure 1 CG representations of the hydraphile molecule and the DMPC lipid are shown. By evoking a CG representation, the number of sites in both the molecules is reduced typically by an order of magnitude compared to their all atom (AA) counterparts. CG models are constructed by using the center of mass position of the corresponding entity in the AA counterpart. Consecutive CG sites in a molecule are bonded by harmonic potential of the form

$$U_{\text{bond}}(r_{ij}) = (k_b/2)(r_{ij} - r_o)^2$$

where the equilibrium bond distance is denoted by r_o and k_b is the bond force constant. The bond angle between three consecutive units in a molecule is determined by the following cosine angle potential,

$$U_{\text{bend}}(\theta_{ijk}) = k_\theta[1 - \cos(\theta_o - \theta_{ijk})]$$

where θ_{ijk} is the bend angle formed by the three sites i, j, and k. More details on the choice of CG representation and parametrization can be found elsewhere.[24] As in the earlier work,[24] water is modeled as a single spherical site corresponding to a loose grouping of three water molecules. Nonbonded CG sites interact via Lennard-Jones potentials of the form

$$U(r_{ij}) = (27/4)\epsilon[(\sigma/r_{ij})^m - (\sigma/r_{ij})^n]$$

where we use $m = 9$ and $n = 6$ for all the species except water. For water we use $m = 6$ and $n = 3$. For certain species tabulated potentials are used.[24] Tabulated potentials between various CG sites used in this study are plotted in Figure 2. All the relevant parameters for the Lennard-Jones interaction are listed in Table 1.

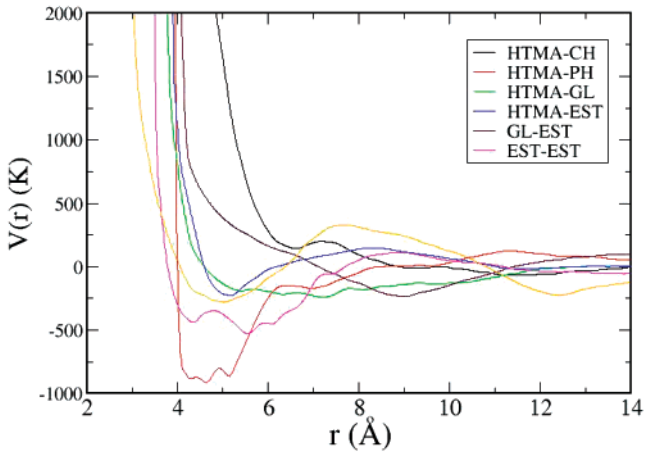

Figure 2. Graphical representation of the tabulated potentials for various interacting CG species shown as a function of distance.

There are three major steps involved in constructing the simulation system: The first involves construction of a lipid bilayer system, the second, the insertion of the hydraphile into lipid bilayer core, and the third, the addition of ions to the aqueous region of the equilibrated lipid bilayer/hydraphile system. In the following we describe each of these steps in more detail.

The lipid simulation system is constructed by replicating a basic unit containing 4 DMPC molecules (2 in the upper leaflet and 2 in the lower leaflet) and 144 CG water molecules. DMPC molecules are placed in such a way that the hydrophobic tails face each other, whereas the hydrophilic headgroups are exposed to water. This system is allowed to relax and equilibrate at 298.15 K in a constant pressure (NPT) ensemble. The molecular dynamics calculations utilize our in-house Center for Molecular Modeling Molecular Dynamics (CM^3D) program,[26] which allows the simulation of a wide variety of ensembles. We then replicated the simulation cell in the *xy*-plane to generate systems with 8, 16, 32, 64, 128, and 256 lipids, respectively. Each of these systems was equilibrated for 5 ns, before generating a larger system. In each case, care has been taken to remove overlapping water molecules. After such delicate adjustments to remove overlapping lipid/water molecules, the final system contains 256 DMPC lipids (128 in each leaflet of the bilayer) and 4602 CG water molecules (recall that in the present representation, each of the CG water site implicitly represents three real water molecules). As before, the simulation system is allowed to relax and equilibrate at 298.15 K for 5 ns. For the next 5 ns the stability of the bilayer is monitored. As mentioned in earlier studies,[24−30] the CG approach involves smooth potentials, which essentially results in effective simulation times that are about 2 orders of magnitude larger in comparison to the corresponding all atom simulation times. The times reported in this article are the actual CG simulation times and not the longer effective times.

To study the hydraphile insertion into lipid bilayer and its channel conformation, a series of the hydraphiles with different

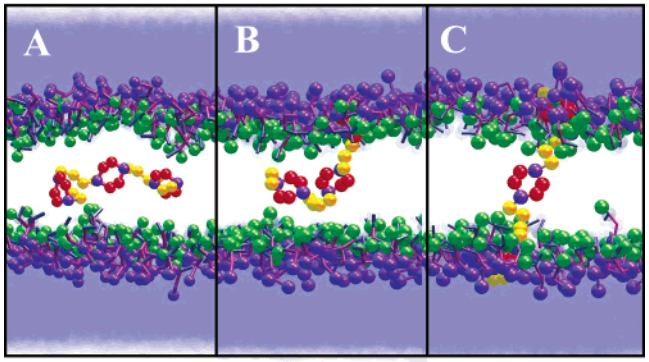

Figure 3. Snapshots of a hydraphile embedded within a DMPC bilayer (A) $t = 0$ ns, (B) 0.25 ns, and (C) 1.7 ns. Lipid tails are not shown for visual clarity. The light blue region represents water, whereas the dark blue and green spheres represent the bilayer headgroup region. The simulation system contains 256 DMPC lipids, 4602 water sites, and a single HY4 hydraphile.

lengths of hydrocarbon chains are constructed. By varying the length of the linking chains, hydraphiles with any desired length can be conveniently constructed. In CG simulations this is achieved by adding or removing hydrocarbon CG units in linking chain. Linking chains with 2, 4, and 6 hydrophobic (SM) units per linking chain are labeled as HY2, HY4, and HY6, respectively. According to the present CG representation each of the SM units in the linking chain adds 0.32 nm to the hydraphile length. Hence, HY2, HY4, and HY6 lengths approximately correspond to 1.92, 3.2, and 4.48 nm, respectively. From the CG simulations the hydrophobic thickness of DMPC bilayer is calculated as 3.0 nm. Hence, among the three hydraphiles, HY4 is the most likely candidate for the ion channel formation.

Different simulations systems are generated by inserting each of these hydraphiles separately into the equilibrated lipid bilayer system by positioning it closer to the overlapping region of two leaflets and parallel to the bilayer plane, as shown in Figure 3A. To avoid the difficulties due to the overlap of the hydraphile with the neighboring lipid tails, we begin the equilibration with a relatively small time step (0.1 fs) and gradually increase the time step to 10 fs over a period of 10^4 steps. At the end, with the 10 fs time step, further equilibration is carried out for 5 ns. To obtain an unbiased starting configuration, the hydraphile is kept immobile during the equilibration process. After the equilibration, the constraints on the hydraphile movement are removed.

By following the procedure described above, three different simulation systems are constructed by inserting HY2, HY4, and HY6 molecules separately into the lipid bilayer. To investigate the postulated membrane-spanning conformation,[15,16] each of these systems is individually studied. To begin with, we have selected the HY4 system as its length roughly matches the bilayer thickness. In the initial conformation, shown in Figure 3A, the interaction of the hydrophobic SM sites with the bilayer core is favorable but the 18-crown-6 rings, being hydrophilic, should tend to diffuse away from the hydrophobic environment toward the polar interface regions. Indeed, during the course of the MD simulation, one of the terminal 18-crown-6 rings rapidly diffused to the (upper) lipid−water interface region (shown in Figure 3B).

The lipid headgroups, being polar in nature, assist the accommodation of the hydrophilic crown-ether ring into the interface region and two rings remain within the hydrophobic core (Figure 3B). At this point, the central ring is unable to reach the other (lower) interface due to insufficient length of

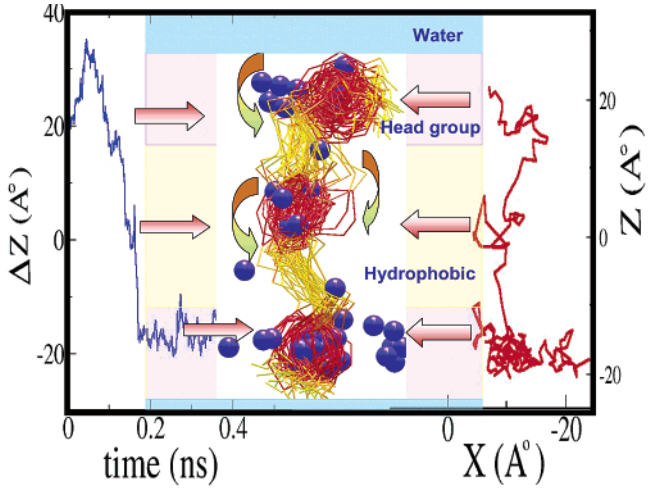

Figure 4. Cation translocation mechanism as observed in the present CG simulation. Left panel: Displacement (Δz) of the ion along the direction of the bilayer normal as a function of time. Middle panel: Overlap of 43 snapshots (each separated by 10 ps) during the ion translocation period. Shown are the hydraphile crown regions (red), hydrocarbon chains (yellow), and sodium ion (blue sphere). The curved arrows indicate the direction of the ion transport. Right panel: The cation trajectory along the transmembrane direction ($X-Z$ plane).

hydrocarbon linker to the ring that has already been accommodated into the (upper) interface. However, the terminal ring can diffuse to find a more suitable environment. There are two possibilities: (a) insertion into the same (upper) interface as the first ring or (b) insertion into the opposite interface. The present simulations suggest that the latter option is more favorable (Figure 3C). In this configuration both terminal crowns are anchored in the polar headgroup regions, whereas the middle ring is relatively free to move. This structure is observed after 1.7 ns and found to be stable throughout the remaining simulation time (45 ns). In this membrane-spanning configuration, the terminal rings could serve to act as entry and exit portals for cations, whereas the middle ring may provide transient stability for the ions crossing the hydrophobic membrane core.[15] Indeed, this is one of the two postulated conformations proposed by Gokel et al.[15,16]

Because our aim is to study the ion translocation across the lipid bilayer, once the hydraphile adopted this membrane-spanning conformation, we introduced six cations into the water phase and continued the MD simulation. Gokel et al. studied the translocation of Na^+ ions across a membrane. Hence we have chosen to employ a CG model of a cation, which resembles the hydrated Na^+ ion. In doing so, we assume the cation is octahedrally hydrated with water.[31−33] Thus, each sodium ion is therefore represented by a single spherical CG (NA) site with a mass modified to reflect the ion and its accompanying solvent sheath water molecules.

After a further 2 ns of simulation, we observed the hydraphile assisted cation translocation. The trajectory of the ion is indicated in Figure 4. The transit time for the ion to be transported from one interface region to the other was approximately 0.22 ns. As shown in Figure 4, the ion resides for a relatively longer time in the end rings before and after it passes through the central ring. Once the ion enters the hydrophobic region, it takes less than 30 ps for it to reach the central relay. On the other hand, the ion is observed to reside 60−70 ps in the central ring (a relatively short time compared to the residence time for the terminal rings, more than 120 ps). The plateaus in the trajectory appear when the ion reaches the crown-ether rings, and are denoted by straight arrows in Figure 4. It can be seen

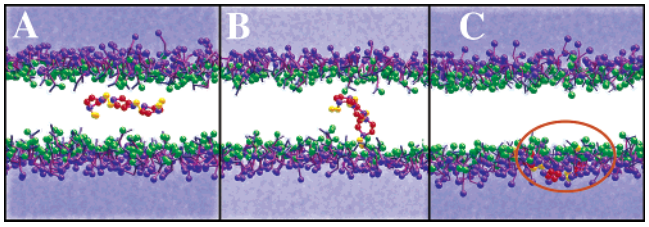

Figure 5. Simulation snapshots of a short hydraphile (HY2) insertion into lipid bilayer. (A) initial conformation ($t = 0$ ns); (B) $t = 0.21$ ns; (C) final conformation. Position of the hydraphile in (C) is highlighted with a circle. As shown in figure, HY2 is too short in length to span the bilayer thickness. Lipid tails and headgroup spheres are not shown for visual clarity (color code is same as that of Figure 3).

that the ion shows relatively less mobility in the vicinity of the hydraphile ring when compared to that in bulk water.

Experimental studies suggested that the existence of the central relay assists ion transport across the membrane because a positive ion cannot traverse a distance of more than 3 nm. Simulations provide a unique way of testing this speculation. To examine this point, we have repeated the above simulation with the hydraphile containing a "neutral" central relay. In simulations this is achieved by switching off the charges on the central relay. In other words, in this case the hydraphile has polar entry portals and a "neutral" central relay. Apart from the polarity, the central relay is the same as that of entry portals. If the polarity of the central relay does not play any role, we expect this case to be no different from the previous simulations. Surprisingly, no ion transport is observed in this case, at least for the length of simulation we have carried out, which was nearly an order of magnitude longer time in this case. Hence, we conclude that the hydraphile with a "neutral" central ring cannot assist the ion transport. Thus, our CG simulations highlight the necessity of the charged central relay for the ion transport.

We proceed to study the experimentally observed[15,16,34] dramatic decrease in the ion transport efficiency when the linker hydrocarbon chain length (either long or short) does not match the bilayer thickness. We have attempted to study the ion transport by inserting the hydraphiles with different lengths. For this purpose we have carried out simulation studies with both HY2 and HY6 similar to those with HY4. Simulation snapshots observed in case of HY2 are shown in Figure 5. Initially, HY2 is placed in the bilayer core region, as shown in Figure 5A. During the course of simulation, HY2 attempts to adopt a channel-like conformation in a fashion similar to that observed for HY4. When the hydraphile reaches one of the bilayer−water interfaces, one of the end rings gets inserted into the headgroup region, as shown in Figure 5B. However, HY2 is too short in length to span the DMPC bilayer core thickness. As a result, all three crowns get immersed into the headgroup region of only one of the interfaces, thereby failing to form a transmembrane structure. This is shown in Figure 5C. On the other hand, HY6, a relatively longer hydraphile, shows different features. The simulation snapshots for HY6 insertion are shown in Figure 6. During the simulation one of the end rings gets inserted into lipid headgroup region, as shown in Figure 6A. As HY6 is longer than bilayer core thickness, in principle it should be able to span the bilayer core region and reach the other interface. Indeed, this is observed and is shown in Figure 6A. However, HY6 is too long in length compared to the bilayer thickness to make a stable membrane-spanning conformation. As a result, HY6 attains a conformation in which both the end rings get inserted into the same interface region, as shown in Figure 6B, leaving the central ring of the hydraphile still in the hydrophobic

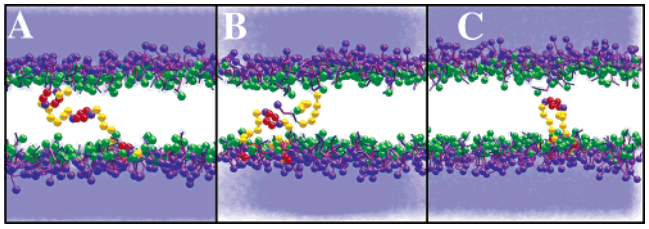

Figure 6. Simulation snapshots of a long hydraphile HY6 in a lipid bilayer: (A) $t = 0$ ns; (B) $t = 0.18$ ns. At this stage, lipids from the nearby interface unsuccessfully try pulling the polar central relay during the insertion process. (C) Final conformation. HY6 has linker chains that are longer than required to match the bilayer thickness, thereby failing to form a transmembrane conformation. Lipid tails and headgroup spheres are not shown for visual clarity. Along with Figure 5, this figure represents the hydrophobic "mismatch" scenario for the hydraphiles that do not match the bilayer thickness (color code is same as in Figure 3).

core region. At this stage, lipid headgroups from the nearby interface interact with the polar central relay, thereby trying to pull the central relay toward the interface. This is shown in Figure 6B. However, the lipids are unsuccessful in doing so, as both the end rings of the hydraphile are already inserted into the other interface region. Note that HY6 is at least 2 times longer in length compared to the DMPC lipid used in this study. Thus, HY6 fails to form a membrane-spanning conformation and attains a final conformation as shown in Figure 6C.

Hence, it can be concluded that the hydraphiles with lengths that are either too long or too short fail to form a transmembrane structure due to the mismatch with the bilayer core thickness. This also explains the experimentally observed relative inefficiency of the hydraphiles to transport ions across a membrane, when there is a mismatch with the bilayer thickness

In conclusion, the application of a coarse grain simulation methodology has allowed us to explore the translocation mechanism associated with the experimentally reported hydraphile assisted cation transport. The CG simulations cover effective time scales of microseconds, which are difficult to achieve with their all-atom counterparts.[22−24] Our simulations confirm that the hydraphile molecule with a chain length matching the bilayer thickness is the most effective at ion transport. The simulation results suggest that the ion channel model proposed by Gokel and co-workers[15,16] is viable. In addition, the present simulation study underscores the necessity of a polar central relay for a molecule to act as a translocation facilitator.

The observed ion translocation across the bilayer is found to be a relatively rare event. Thus, to obtain statistically meaningful information, many simulations are required. Unfortunately, even with the CG technique employed in this work, carrying out a large number of such rare event simulations is computationally expensive with the typical resources available today. Despite such limitations, the present study was able to shed light on the mechanism of hydraphile assisted ion translocation across a lipid bilayer. By using this CG methodology one should be able to model other synthetic channels and we plan to extend the present methodology to handle such problems.

Acknowledgment. We thank Steve Nielsen, Preston Moore, and John Shelley for their interest and help. This research was sponsored by the National Science Foundation and the National Institutes of Health.

Supporting Information Available: Bond and bend interaction parameters for the CG sites used in this study, mass density profiles, and a movie file are available free of charge at http://pubs.acs.org.

References and Notes

(1) Zhou, M.; Morais-Cabral, J. H.; Mann, S.; MacKinnon, R. *Nature* **2001**, *411*, 657. Zhou, Y.; Morais Cabral, J. H.; Kaufman, A.; MacKinnon, R. *Nature* **2001**, *414*, 43.

(2) Hille, B. *Ion Channels of Excitable Membranes*; Sinauer Associates: Sunderland, MA, 2001.

(3) Miyazawa, A.; Fujiyoshi, Y.; Unwin, N. *Nature* **2003**, *423*, 949−955. Unwin, N. *Nature* **1995**, *373*, 37−43.

(4) Schonwetter, B.; Stolzenberg, E. D.; Zasloff M. A. *Science* **1995**, *207*, 1645−1648. Zasloff, M. *Nature* **2002**, *415*, 389−395.

(5) Shai, Y. *Biopolymers (Peptide Sci.)* **2002**, *66*, 236−248;

(6) Nizet, X *et al. Nature* **2001**, *414*, 454−456.

(7) Yang, L.; Harroun, T. A.; Weiss, T. M.; Diang, L.; Huang, H. W. *Biophys. J.* **2001**, *81*, 1475−1485.

(8) DeGrado W. F.; Lear J. D.; Wasserman Z. R. *Science* **1989**, *243*, 622−628.

(9) Epand, R. F.; Umezawa, N.; Porter, E. A.; Gellman, S. H.; Epand, R. M. *Eur. J. Biochem.* **2003**, *270*, 1240−1248.

(10) Das, S.; Lengeweiler, U. D.; Seebach, D.; Reusch, R. N. *Proc. Natl. Acad. Sci. U.S.A.* **1997**, *94*, 9075−9079.

(11) Clark, T. D.; Buehler, L. K.; Ghadiri, M. R. *J. Am. Chem. Soc.* **1998**, *120*, 651−656.

(12) Lin, V. S.-Y.; Motesharei, K.; Dancil, K.-P. S.; Sailor, M. J.; Ghadiri, M. R. *Science* **1997**, *278*, 840−843.

(13) Hamuro, Y.; Schneider, J. P.; DeGrado, W. F. *J. Am. Chem. Soc.* **1999**, *121*, 12200−12201.

(14) Tew, G. N.; Liu, D.; Chen, B.; Doerksen, R.; Kaplan, J.; Carroll, X.; Klein, M. L.; DeGrado, W. F. *Proc. Natl. Acad. Sci.* **2002**, *99*, 5110−5114.

(15) Leevy, W. M.; Donato, G. M.; Ferdani, R.; Goldman, W. E.; Schlesinger, P. H.; Gokel, G. W. *J. Am. Chem. Soc.* **2002**, *124*, 9022−9023.

(16) Gokel, G. W.; Mukhopadyay, A. *Chem. Soc. Rev.* **2001**, *30*, 274−286. (c) Gokel, G. W. *Chem. Commun*. **2000**, 1−9.

(17) Elber, R.; Gosh. A.; Cardenas, A. *Acc. Chem. Res.* **2002**, *35*, 396−403.

(18) Gosh A.; Elber, R.; Scheraga, H. A.; *Proc. Natl. Acad. Sci. U.S.A.* **2002**, *99*, 10394−10398.

(19) Zhong, Q.; Jiang, Q., Moore P. B.; Newns, D. M.; Klein M. L. *Biophys. J.* **1998**, *74*, 3−10.

(20) Cheng, Y.-K.; Sheu, W.-S.; Rossky, P. J. *Biophys. J.* **1999**, *76*, 1734−1743.

(21) Balasubramanian, S. and Bagchi, B.; *J. Phys. Chem. B* **2002**, *106*, 3668. Balasubramanian, S.; Pal, S.; Bagchi, B.; *Phys. Rev. Lett.* **2002**, *89*, 115505.

(22) Smit, B.; Hilbers, P. A. J.; Esselink, K.; Rupert, L. A. M.; Van Os, N. M.; Schlijper, A. G. *J. Phys. Chem.* **1991**, *95*, 6361.

(23) Goetz, R.; Gompper, G.; Lipowsky, R. *Phys. Rev. Lett.* **1999**, *82*, 221.

(24) Shelley, J. C.; Shelley, M. Y.; Reeder, R. C.; Bandyopadhyay, S.; Klein, M. L. *J. Phys. Chem. B* **2001**, *105*, 4464−4470.

(25) Lopez C. F.; Moore P. B.; Shelley, J. C.; Shelley M. Y.; Klein M. L.; *Comput. Phys. Comm.* **2002**, *147*, 1−6.

(26) Nielsen, S.; Klein, M. L. In *Bridging time scales: Molecular simulations for the next decade*; Nielaba, P., Mareschali, M., Ciccotti, G., Nielsen, S., Lopez, C. F., Srinivas, G., Klein, M. L. *J. Chem. Phys.* **2003**, *119*, 7043.

(27) Marrink, S. J.; Mark, A. E. *J. Am. Chem. Soc.* **2003**, ASAP ja036138;

(28) Tieleman, D. P.; Leontiadou, H.; Mark, A. E.; Marrink, S. J. *J. Am. Chem. Soc.* **2003**, *125*, 6382.

(29) Marrink S. J.; Lindahl, E, Edholm, E.; Mark A. E. *J. Am. Chem. Soc.* **2001**, *123*, 8638.

(30) Marrink, S. J.; Mark A. E. *J. Phys. Chem. B* **2001**, *105*, 6122.

(31) Lopez, S. F.; et al. *Nature* **2001**, *412*, 452−455.

(32) Beven, L.; Helluin, O.; Molle, G.; Ducloheir, H.; Wroblewski, H. *Biochim, Biophys. Acta* **1999**, *1421*, 53−63;

(33) Morais-Cabral, J. H.; Zhou, Y.; Mackinnon, R. *Nature* **2001**, *414*, 37.

(34) Angelova, A.; Ivonov, R.; Koch, M. H. J.; Rapp, G. *Bulg. Arch. Biochem. Biophys.* **2000**, *378*, 93−106.